PROCEEDINGS OF SCIENCE

Investigation of Multi-Messenger Properties of FR0 Radio Galaxy Emitted Ultra-High Energy Cosmic Rays

J.P. Lundquist,[1,*] **L. Merten,**[2,3] **S. Vorobiov,**[1] **M. Boughelilba,**[4] **A. Reimer,**[4] **P. Da Vela,**[4] **F. Tavecchio,**[5] **G. Bonnoli**[5] **and C. Righi**[5]

[1] *Center for Astrophysics and Cosmology (CAC), University of Nova Gorica, Vipavska 13, SI-5000 Nova Gorica, Slovenia*

[2] *Theoretical Physics IV, Plasma Astroparticle Physics, Faculty for Physics and Astronomy, Ruhr University Bochum, 44780 Bochum, Germany*

[3] *Ruhr Astroparticle and Plasma Physics Center (RAPP Center), Germany*

[4] *Universität Innsbruck, Institut für Astro- und Teilchenphysik, Technikerstraße 25/8, 6020 Innsbruck, Austria*

[5] *Astronomical Observatory of Brera, Via Brera 28, 20121 Milano, Italy*

E-mail: jplundquist@gmail.com

Low luminosity Fanaroff-Riley type 0 (FR0) radio galaxies are amongst potential contributors to the observed flux of ultra-high energy cosmic rays (UHECRs) [1]. Due to FR0s' much higher abundance in the local universe than more powerful radio galaxies (e.g., about five times more ubiquitous at redshifts $z \leq 0.05$ than FR1s), they could provide a substantial fraction of the total UHECR energy density [2].

In the presented work, we determine the mass composition and energy spectrum of UHECRs emitted by FR0 sources by fitting simulation results from the CRPropa3 framework [3] to the recently published Pierre Auger Observatory data (Auger) [4, 5]. The resulting emission spectral characteristics (spectral indices, rigidity cutoffs) and elemental group fractions are compared to the Auger results. The FR0 simulations include the approximately isotropic distribution of FR0s extrapolated from the measured FR0 galaxy properties and various extragalactic magnetic field configurations, including random and large-scale structured fields. We predict the fluxes of secondary photons and neutrinos produced during UHECR propagation through cosmic photon backgrounds. The presented results allow for probing the properties of the FR0 radio galaxies as cosmic-ray sources using observational high-energy multi-messenger data.

XVIII International Conference on Topics in Astroparticle and Underground Physics (TAUP2023)
28.08-01.09.2023
University of Vienna

[*] Speaker

PoS(TAUP2023)134

1. Methodology

The CRPropa3 [3, 6] framework is used to simulate ultra-high energy cosmic ray (UHECR) proton, helium, nitrogen, silicon, and iron propagation through the intergalactic medium. Interactions with photon backgrounds CMB, IRB, and URB, redshift adiabatic cooling, and nuclear decays are accounted for. The simulations are extrapolated from the 76 FR0s in FR0CAT [2] (+/-45°SGB, 60°to 120°SGL, $z < 0.05$), resulting in 645 simulated FR0 with an isotropic pointing-direction while maintaining the proper redshift distribution and a relative flux proportional to radio output. The correlation between radio output/UHECR flux and redshift is also preserved to model source evolution [2]. Further details on the simulations and the following fit results can be found in Ref. [7].

Four magnetic field models and the no field case are compared. Two of the magnetic fields are 1 nG Kolmogorov spectrum turbulent fields with correlation lengths of 234 kpc (Rand. A) and 647 kpc (Rand. B). The third and fourth models are the Dolag et al. [8] (0.047 nG) and Hackstein et al. (CLUES) 'astrophysical1R' (0.064 nG) structured magnetic fields [9].

To find the FR0 UHECR combined composition/spectrum emission best matching Auger data [4, 5], we minimize the sum χ^2/dof for composition and energy spectrum via the eight parameters of observed nucleon fractions, emission spectral index γ, rigidity-dependent exponential emission cutoff [10], maximum particle trajectory cutoff, and the observed relative spectrum normalization. Uncertainties on the fitting method, data statistics, and systematics (reported as 68.27% best-fit value confidence intervals) are accounted for by bootstrap sampling simulations and sample adjusting data with random Gaussian offsets using the total systematic/statistical uncertainties.

2. Results

Figure 1 shows combined fits to the composition and energy spectrum for the five magnetic field configurations and two extensive air-shower (EAS) models (EPOS-LHC and QGSJETII-04) compared to data. For the mean log mass number, $\langle \ln A \rangle$, the 1 nG random fields have the best fit to the low energy bins. No model accounts for the highest energy bin of the energy spectrum, therefore FR0 are not expected to significantly contribute to the most extreme energy events.

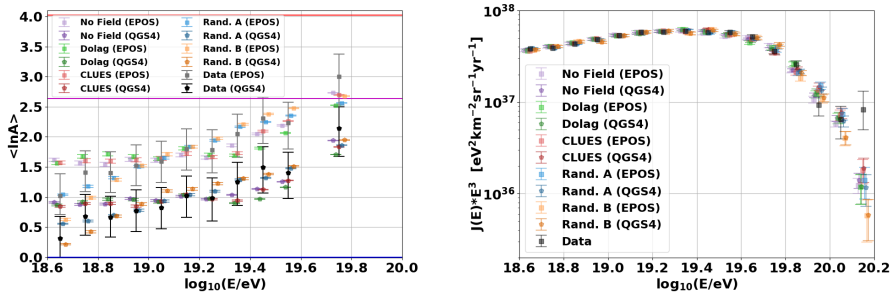

Figure 1: Combined fits of UHECR composition and energy spectrum for all 10 models. (a) Mean log mass number $\langle \ln A \rangle$ for data/fits. Lines are blue:H, magenta:He, and red:Fe. (b) J*E^3 energy spectra for data/fits.

Table 1 shows each fit's $\Sigma\chi^2$/dof, spectral index (γ), rigidity cutoff ($\log_{10}(R_{\rm cut})$), trajectory cutoff ($D_{\rm cut}$), and spectrum norm. (n). The best fits are Rand. A (best overall for either EAS model), no field, and CLUES. QGSJETII-04 has a worse goodness-of-fit more often than EPOS-LHC.

Field	Model	$\Sigma\chi^2$/dof	γ	$\log_{10}(R_{cut})$	D_{cut}	n
No Field	EPOS	3.007	$2.57^{+0.03}_{-0.08}$	$19.34^{+0.15}_{-0.06}$	219^{+0}_{-0}	$1.335^{+0.009}_{-0.004}$
	QGS4	3.916	$2.58^{+0.02}_{-0.02}$	$19.42^{+0.03}_{-0.02}$	219^{+0}_{-0}	$1.339^{+0.005}_{-0.004}$
Dolag	EPOS	4.430	$2.63^{+0.02}_{-0.11}$	$19.43^{+0.06}_{-0.12}$	226^{+15}_{-0}	$1.335^{+0.008}_{-0.007}$
	QGS4	4.304	$2.60^{+0.04}_{-0.04}$	$19.48^{+0.04}_{-0.03}$	230^{+17}_{-4}	$1.341^{+0.005}_{-0.004}$
CLUES	EPOS	3.178	$2.63^{+0.04}_{-0.07}$	$19.37^{+0.06}_{-0.07}$	219^{+0}_{-0}	$1.333^{+0.009}_{-0.004}$
	QGS4	3.774	$2.65^{+0.02}_{-0.05}$	$19.45^{+0.04}_{-0.02}$	219^{+0}_{-1}	$1.341^{+0.005}_{-0.006}$
Rand.A	EPOS	2.010	$2.67^{+0.22}_{-0.12}$	$19.57^{+0.18}_{-0.04}$	424.0^{+111}_{-191}	$1.342^{+0.005}_{-0.003}$
	QGS4	1.965	$2.64^{+0.10}_{-0.15}$	$19.54^{+0.03}_{-0.06}$	256^{+161}_{-28}	$1.342^{+0.005}_{-0.004}$
Rand.B	EPOS	4.314	$2.92^{+0.14}_{-0.30}$	$19.62^{+0.49}_{-0.05}$	401^{+83}_{-116}	$1.345^{+0.005}_{-0.005}$
	QGS4	4.472	$2.80^{+0.11}_{-0.11}$	$19.58^{+0.07}_{-0.04}$	281^{+36}_{-49}	$1.344^{+0.006}_{-0.003}$

Table 1: FR0 emission combined fit results for all 10 models. Goodness-of-fit $\Sigma\chi^2$/dof, spectral index (γ), rigidity cutoff ($R_{\rm cut}$), trajectory cutoff ($D_{\rm cut}$), and relative spectrum normalization (n).

The emission spectral index, γ, tends to increase with magnetic field strength – and is generally softer for QGSJETII-04 due to lighter nuclei. The rigidity cutoff ($R_{\rm cut}$) and propagation trajectory cutoff ($D_{\rm cut}$) tend to increase with field strength. The spectrum normalization also tends to increase with field strength and is generally larger for QGSJETII-04 (due to spallation for the heavier EPOS-LHC nucleons) which suggests the highest energy CRs emitted must increase with magnetic field strength.

The FR0 nucleon emission fractions are listed in Table 2. As magnetic field strength increases, the proton fraction is relatively stable, helium and nitrogen fractions tend to increase, while the number of heavier nuclei tend to decrease. This is likely heavier nuclei having longer trajectories due deflection increasing with magnetic field strength, resulting in an increase of spallation secondaries.

Field	Model	f_H(%)	f_{He}(%)	f_N(%)	f_{Si}(%)	f_{Fe}(%)
No Field	EPOS	$90.0^{+1.2}_{-4.6}$	$0.0^{+1.9}_{-0.0}$	$0.0^{+0.0}_{-0.0}$	$8.7^{+3.0}_{-1.6}$	$1.3^{+0.3}_{-0.5}$
	QGS4	$96.4^{+0.7}_{-1.9}$	$0.0^{+0.9}_{-0.0}$	$0.0^{+0.0}_{-0.0}$	$2.5^{+0.8}_{-1.1}$	$1.1^{+0.3}_{-0.2}$
Dolag	EPOS	$91.8^{+1.6}_{-5.8}$	$0.6^{+5.1}_{-0.6}$	$0.0^{+0.0}_{-0.0}$	$5.4^{+2.4}_{-1.6}$	$2.2^{+0.6}_{-0.8}$
	QGS4	$93.3^{+4.2}_{-4.9}$	$4.2^{+4.7}_{-4.2}$	$0.0^{+0.0}_{-0.0}$	$1.0^{+0.7}_{-0.8}$	$1.5^{+0.4}_{-0.3}$
CLUES	EPOS	$92.3^{+1.0}_{-2.8}$	$0.0^{+0.7}_{-0.0}$	$0.0^{+0.0}_{-0.0}$	$5.9^{+1.6}_{-1.3}$	$1.8^{+0.4}_{-0.6}$
	QGS4	$97.4^{+0.3}_{-4.0}$	$0.0^{+3.6}_{-0.0}$	$0.0^{+0.0}_{-0.0}$	$1.2^{+0.8}_{-0.7}$	$1.4^{+0.2}_{-0.3}$
Rand.A	EPOS	$71.7^{+13.9}_{-21.0}$	$19.5^{+19.9}_{-0.0}$	$6.6^{+2.9}_{-2.6}$	$1.2^{+1.1}_{-0.6}$	$1.0^{+0.3}_{-0.6}$
	QGS4	$83.7^{+9.4}_{-8.4}$	$13.0^{+8.9}_{-10.7}$	$2.4^{+1.3}_{-1.4}$	$0.6^{+0.3}_{-0.6}$	$0.3^{+0.2}_{-0.0}$
Rand.B	EPOS	$89.6^{+1.3}_{-89.6}$	$0.6^{+86.4}_{-0.6}$	$8.5^{+1.7}_{-3.0}$	$0.9^{+2.9}_{-0.3}$	$0.4^{+0.2}_{-0.1}$
	QGS4	$95.3^{+0.8}_{-0.8}$	$0.0^{+0.0}_{-0.0}$	$4.2^{+0.5}_{-1.0}$	$0.3^{+0.3}_{-0.2}$	$0.1^{+0.0}_{-0.1}$

Table 2: The FR0 combined fit results nucleon emission percentages for proton (f_H), helium (f_{He}), nitrogen (f_N), silicon (f_{Si}), and iron (f_{Fe}) primaries for all 10 models.

Cosmogenic integral photon [11] and all-flavor neutrino spectra [12–14] are shown in Figure 2 for the best fit model – Rand. A magnetic field and QGSJETII-04 composition. This light nucleon emission results in an integral photon flux largely compatible with the pure proton GZK production prediction. The neutrino flux is similar to a pure iron prediction which may be partially due to the relatively close sources simulated (z<0.05). Given the range of theoretical predictions and experimental limits the simulated FR0 flux is reasonable. Overall, the larger magnetic fields result in larger cosmogenic fluxes of photons and neutrinos.

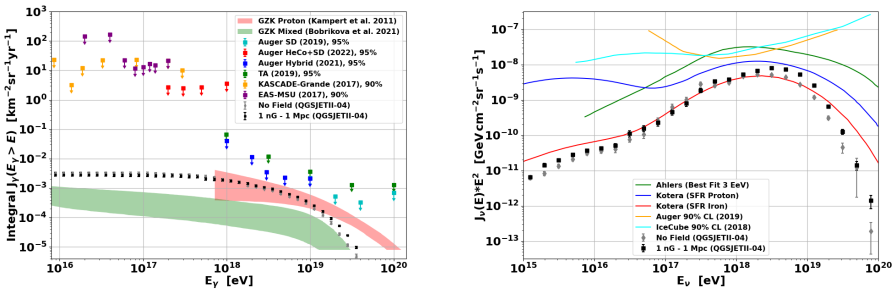

(a) **(b)**

Figure 2: FR0 best fit (Rand.A, QGSJETII-04) cosmogenic multi-messenger spectra with upper limits from various experiments and theoretical predictions. (a) Integral photon spectrum. (b) Neutrino spectrum J*E^2.

3. Conclusion

Nearby isotropic FR0 radio galaxy (z<0.05) emission aligns well with the Auger UHECR composition, for two popular air-shower models (EPOS-LHC and QGSJETII-04), and the energy spectrum [4, 5]. Our results indicate a soft, largely protonic emission spectrum (γ~-2.6) and reasonable cosmogenic photon and neutrino fluxes. This work underscores a potential linkage between FR0 radio galaxies and a large fraction of UHECRs, shedding light on UHECR origins and interactions within the intergalactic medium. Future research may consider FR0 sources at larger redshifts (z>0.05), additional shower models, and assess the CR luminosity of FR0s.

Acknowledgements

Financial support received from the grant numbers I 4144-N27 (FWF), N1-0111 (ARRS), SFB1491 (DFG), 847476 (EU). Further acknowledgment information can be found in Ref. [7]

References

[1] Merten, L. *et al.*, Astroparticle Physics, 128 (2021) 102564.
[2] Baldi, R. D., Capetti, A., Massaro, F., Astron. Astrophys. 609 (2018) A1.
[3] Alves Batista, R. *et al.*, JCAP 05 (2016) 038.
[4] Yushkov, A. on behalf of the Pierre Auger Collaboration, PoS ICRC2019 (2020) 482.
[5] Deligny, O., PoS ICRC2019 (2020) 234.
[6] Merten, L., Becker Tjus, J. , Fichtner, H., Eichmann, B., Sigl, G., JCAP 2017 (6) (2017) 046.
[7] Lundquist, J.P., *et al.*, PoS ICRC2019 (2023) 1512.
[8] Dolag, K., Grasso, D., Springel, V., Tkachev, I., JCAP 01 (2005) 009.
[9] Hackstein, S. *et al.*, Mon. Not. Roy. Astron. Soc. 475 (2) (2018) 2519–2529.
[10] Aab, A., *et al.*, JCAP 04 (2017) 038, [Erratum: JCAP 03, E02 (2018)].
[11] Abreu, P., *et al.*, The Pierre Auger Collaboration, Astrophys. J. 933 (2) (2022) 125.
[12] Aartsen, M. G., *et al.*, Phys. Rev. D 98 (6) (2018) 062003.
[13] Aab, A., *et al.*, JCAP 10 (2019) 022.
[14] Kotera, K., Allard, D., Olinto, A. V., JCAP 2010 (10) (2010) 013.